Environmental Science & Technology

ARTICLE

pubs.acs.org/est

Greenhouse Gas Emissions from Operating Reserves Used to Backup Large-Scale Wind Power

Matthias Fripp*

Environmental Change Institute, University of Oxford, South Parks Road, Oxford, OX2 3QY, United Kingdom

Supporting Information

ABSTRACT: Wind farms provide electricity with no direct emissions. However, their output cannot be forecasted perfectly, even a short time ahead. Consequently, power systems with large amounts of wind power may need to keep extra fossil-fired generators turned on and ready to provide power if wind farm output drops unexpectedly. In this work, I introduce a new model for estimating the uncertainty in short-term wind power forecasts, and how this uncertainty varies as wind power is aggregated over larger regions. I then use this model to estimate the reserve requirements in order to compensate for wind forecast errors to a 99.999% level of reliability, and an upper limit on the amount of carbon dioxide that would be emitted if natural gas power plants are used for this purpose. I find that for regions larger than 500 km across, operating reserves will undo 6% or less of the greenhouse gas emission savings that would otherwise be expected from wind power.

1. INTRODUCTION

Forecasts of electricity production from wind farms are uncertain, even an hour or less ahead. Conventional power plants require time to start up and begin delivering power to the electric grid, so system operators must turn on extra reserve capacity in advance, to provide power if the output from wind farms falls below the forecast. Alternatively, wind production could rise above the forecast, leaving additional conventional capacity online but unused. Both types of online, idle power plants could consume significant amounts of fuel, causing substantial greenhouse gas emissions, and reversing some of the emission savings that would otherwise be expected from wind power.

Several studies have concluded that little or no additional reserves would be needed to integrate wind power meeting 10−30% of loads in large power systems.[1−6] However, most of these studies have not looked closely at the possibility of large, very rare errors in wind power forecasts. Some assess the uncertainty of wind forecasts made during a 1−3 year period,[1−3] which is not long enough to achieve the 1-in-10-year reliability level often sought by the power industry. Others [4−6] assume that wind power forecast errors can be modeled with a Gaussian distribution, using the standard deviation of errors during a 1−3 year period. However, wind forecast errors often follow a thicker-tailed, non-Gaussian distribution,[7] so this approach can underestimate the likelihood of large errors.

In this work, I introduce a new model for estimating the distribution of errors in short-term, regional wind power forecasts. This model could be used to improve large-scale wind integration studies, but in this work, I use it for a simpler example, estimating the emissions that would occur if gas-fired reserves were used to compensate directly for 99.999% of wind forecast errors in regions of various sizes.

This example serves to set an upper limit on the emissions that could occur when firming up wind power using natural gas power plants. Power systems already carry significant reserves to compensate for errors in electricity load forecasts or unexpected power plant outages. Wind forecast errors are mostly independent of these other sources of uncertainty, and many power systems already have substantial surplus reserves. Consequently, if wind farms provide a small to moderate share of a system's power, existing reserves will be able to compensate for most wind forecast errors, and only a small amount of additional reserves will be required—much less than if dedicated reserves were used to backup the wind separately. However, if wind is added in much larger amounts, then its uncertainty could begin to dominate over the other sources, and the incremental reserve requirements would asymptotically approach (but never exceed) the reserves that would be required to backup wind separately.[1,8]

Katzenstein and Apt [9] estimated the emissions from backing up wind farms in this way using natural gas plants, but they assumed that wind farms would be backed up 100% by natural gas power plants at all times. Their approach makes no use of wind power forecasts or geographic aggregation, and implicitly assumes that wind power output could drop to zero at any time. Mills et al. [10] pointed out that some backup plants could be turned off entirely when wind power forecasts indicate that they are not needed. However, they did not investigate how closely operating reserves could be tailored to the wind forecast without risking shortfalls in electricity production. The power system model introduced in the second half of this work investigates this possibility further.

The example given here focuses on two types of natural gas power plants with startup times of an hour or less, and correspondingly short forecast horizons. This could represent a power system with large shares of gas and wind power (but no hydroelectric or demand-response capability), or a tranche of power provided by gas and wind in a system that contains other,

Received: February 7, 2011
Accepted: July 28, 2011
Revised: June 14, 2011
Published: July 28, 2011

less-flexible resources. Large scale wind may be difficult to develop in power systems with large shares of coal or nuclear power, partly because those resources are not economically or technically suited to ramping up and down to complement wind, and partly because power systems seeking low emissions may switch from coal to gas power at the same time as they adopt large shares of wind power. The models shown here could be readily extended to apply to power systems with additional technologies and forecast horizons (e.g., coal plants committed 24 h or more in advance).

2. WIND FORECAST ERROR SIMULATION MODEL

Because there is a delay between the time when a conventional power plant is committed (given the order to startup) and when it can be dispatched (deliver power on-demand), power system operators must commit plants based on an advance forecast of the amount of power that will be needed. They must also commit extra capacity in case this forecast is incorrect.

In the power system model presented below, combined cycle natural gas plants (CC capacity) are committed based on a regional wind forecast 60 min before power is needed ($t-60$ min), and then simple cycle combustion turbines (CT capacity) are committed at $t-20$ min. Consequently, the performance of the power system depends on two random variables: the changes in the regional wind forecast from time $t-60$ to $t-20$ and from $t-20$ to t. The first of these variables determines how much CT capacity must be committed at $t-20$, to "true up" for errors in the $t-60$ forecast. The second variable determines whether the capacity committed at time $t-20$ is sufficient to prevent a generation shortfall at time t.

The wind forecast error model described below simulates samples from the joint distribution of these two random variables at multiple independent time steps. It first specifies the probability distributions for forecast errors at hypothetical wind farm sites, and the correlation between those sites, based on statistical data from 10 existing wind farms. Then it randomly samples from these distributions to simulate the forecast errors that could occur at the hypothetical wind farms. In Section 3, these simulated forecast errors are used to set appropriate reserve margins for wind dispersed across various-sized geographic regions, and to estimate the carbon dioxide emissions when natural gas plants are used to correct for the wind forecast errors.

2.1. Wind Model Definitions. As discussed above, the key variables governing operation of the power system model below are the changes in the wind forecast from time $t-60$ to $t-20$ and from $t-20$ to t. I identify these random variables as $\Delta_{t,40}$ and $\Delta_{t,20}$, respectively:

$$\Delta_{t,40} \equiv F_{t,20} - F_{t,60}$$

$$\Delta_{t,20} \equiv W_t - F_{t,20}$$

where $F_{t,h}$ is the forecast of total output from all the wind farms in a region at time t (expressed in minutes), made h minutes earlier, and W_t is the total output from all wind farms at time t. Both $F_{t,h}$ and W_t are expressed as "capacity factors," i.e., fractions relative to the total rated capacity (maximum possible output) of all wind farms in the region.

The regional forecast $F_{t,h}$ and regional power output W_t are defined as the weighted sum of forecasts ($f_{i,t,h}$) of power output ($w_{i,t}$) at individual wind farms:

$$F_{t,h} \equiv \sum_i f_{i,t,h} z_i / \sum_i z_i$$

$$W_t \equiv \sum_i w_{i,t} z_i / \sum_i z_i$$

where i indexes over all wind farms in the power system and z_i is the rated capacity (maximum possible power output) of wind farm i (in MW).

It is also helpful to define forecast error variables for individual sites, analogous to the variables used for the whole region:

$$\delta_{i,t,40} \equiv f_{i,t,20} - f_{i,t,60}$$

$$\delta_{i,t,20} \equiv w_{i,t} - f_{i,t,20}$$

With these definitions, the region-wide forecast errors are simply the weighted sum of forecast errors at individual wind farms:

$$\Delta_{t,40} = \sum_i \delta_{i,t,40}\, z_i / \sum_i z_i \quad (1)$$

$$\Delta_{t,20} = \sum_i \delta_{i,t,20}\, z_i / \sum_i z_i \quad (2)$$

For this work, I assume that the individual wind farm forecasts $f_{i,t,h}$ are based on "persistence." This is the simplest possible forecasting method, assuming simply that wind power output will stay constant at the current level. Although other methods may be able to improve on persistence forecasts (especially for horizons longer than a few hours), this method is always available. Consequently, it provides an upper bound on forecast uncertainty. (The model could also be used with other forecasting methods.)

Persistence forecasting gives the following relations:

$$f_{i,t,h} = w_{i,t-h}$$

$$\delta_{i,t,40} = f_{i,t,20} - f_{i,t,60} = w_{i,t-20} - w_{i,t-60} \quad (3)$$

$$\delta_{i,t,20} = w_{i,t} - f_{i,t,20} = w_{i,t} - w_{i,t-20} \quad (4)$$

In this case, $\Delta_{t,40}$ simply shows how much the wind changes between 60 min before the time when electricity is needed and 20 min before. Then $\Delta_{t,20}$ shows the change in wind power output during the last 20 min before electricity is needed. The sum of the two shows the change in wind power during the full hour before electricity is needed.

2.2. Simulation of Wind Power Forecast Errors. The wind error model simulates samples from the joint distribution of $\Delta_{t,40}$ and $\Delta_{t,20}$, for arbitrary collections of hypothetical wind farms. This simulation begins by assigning marginal probability distributions for $\delta_{i,t,40}$ and $\delta_{i,t,20}$ to individual hypothetical wind farms, based on historical data from 10 real wind farms. Correlated random draws from these distributions are then used to represent simultaneous errors of each type at each site. Finally, the errors at individual wind farms are combined to create samples of region-wide forecast errors ($\Delta_{t,40}$ and $\Delta_{t,20}$). These steps are repeated for many independent time steps, t.

The core of this method is the creation of correlated random draws from the probability distributions for the hypothetical wind farms. For each time step t, these are generated in two steps: First (in a system with n hypothetical wind farms), $2n$ variables are generated with uniform marginal distributions between 0 and 1,

and a correlation matrix R_s. Next, these uniform variables are transformed to match the assigned distributions of $\delta_{i,t,40}$ and $\delta_{i,t,20}$ for each wind farm. The second step is done via inverse transform sampling, in which the uniform variables are treated as ranks of the wind farm error distributions, and used to select quantiles from those distributions. The transformed variables have the assigned marginal probability distributions, and by definition their ranks have a correlation matrix equal to R_s (in other words, their Spearman's rank correlation is equal to R_s). In this simulation, R_s is assigned a priori to match the rank correlation expected for the hypothetical wind farms, based on the distance between them.

Specifically, the simulation proceeds via these steps:

Gather statistics from real wind farms:

(1) Empirical values of $\delta_{m,t,40}$ and $\delta_{m,t,20}$ are calculated for each of ten active wind farms, using eqs 3 and 4 with power production data for each minute of the year from July 2008 through June 2009. These calculations exclude periods when the wind farm was curtailed or data was unavailable. (More details on the wind farms and curtailments are given in the Supporting Information.)

(2) The marginal empirical cumulative density functions of $\delta_{m,40}$ and $\delta_{m,20}$ are tabulated for each of the 10 wind farms (indexed by m). These functions, $\hat{F}_{m,40}(x)$ and $\hat{F}_{m,20}(x)$, show the fraction of the time when the forecast error $\delta_{m,40}$ or $\delta_{m,20}$ for each wind farm m is less than or equal to x, where x can range from -1 to 1. The inverse of these functions will later be used to convert uniform variables into variables with the appropriate distribution.

(3) The following information is tabulated for each pair of wind farms (m and n) chosen from among the 10 wind farms (55 unique pairs, including pairing each wind farm with itself):
   (a) distance between the two wind farms in kilometers ($d_{m,n}$),
   (b) Spearman's rank correlation between $\delta_{m,40}$ and $\delta_{n,40}$ ($r_s(\delta_{m,40}, \delta_{n,40})$),
   (c) Spearman's rank correlation between $\delta_{m,20}$ and $\delta_{n,20}$ ($r_s(\delta_{m,20}, \delta_{n,20})$), and
   (d) Spearman's rank correlation between $\delta_{m,40}$ and $\delta_{n,20}$ ($r_s(\delta_{m,40}, \delta_{n,20})$).

   The rank correlations are calculated based on all periods when data were available for both of the paired wind farms. These distances and rank correlations are shown in Figure SI.2 of the SI.

Define the statistical properties for hypothetical wind farms

(4) A set of "virtual" wind farms is defined for analysis. Each wind farm is described by its rated output z_i and location. These can correspond to existing or proposed wind farms in a power system.

(5) Each virtual wind farm i is assigned randomly to have the same marginal distributions of δ_{40} and δ_{20} as one of the ten real wind farms m:

$$F_{i,40}(x) \equiv \hat{F}_{m,40}(x)$$
$$F_{i,20}(x) \equiv \hat{F}_{m,20}(x)$$

(6) Tables are made showing the expected rank correlation between the error variables at every possible pair of virtual wind farms i and j ($r_s(\delta_{i,40}, \delta_{j,40})$, $r_s(\delta_{i,20}, \delta_{j,20})$ and $r_s(\delta_{i,40}, \delta_{j,20})$), based on the distance between the two wind farms. The expected rank correlations are derived from the rank correlations at the real wind farms via linear interpolation among the values collected in step 3. This is equivalent to choosing rank correlations for sites d km apart by reading the value for distance d from one of the straight lines shown in Figure SI.2 of the SI.

(7) The tables from step 6 are assembled into a single large matrix, R_s, showing the expected rank correlation between every pair of wind farms, for both error statistics, i.e., the expected correlation matrix for the vector $[F_{1,40}(\delta_{1,40}), ..., F_{n,40}(\delta_{n,40}) \mid F_{1,20}(\delta_{1,20}), ..., F_{n,20}(\delta_{n,20})]$, for wind farms 1...$n$.

(8) R_s is not guaranteed to be a valid correlation matrix (in particular, positive definite), so it is adjusted using the algorithm proposed by Higham.[11] This adjustment produces a matrix very similar to the original one, with around 0.999 correlation between the terms of the two matrices.

Generate data with the specified statistical properties:

(9) The methods described by Li and Hammond [12] are used to simulate random variables with uniform marginal distributions on $[0, 1]$, and the correlation structure defined in step 7. There are $2n$ such variables: $u_{1,t,40}$, ..., $u_{n,t,40}$, $u_{1,t,20}$, ..., $u_{n,t,20}$. These variables are simulated repeatedly for many time steps; $1 \le t \le 10^7$ for each scenario reported in this work.

(10) Forecast errors for each site i are calculated from the simulated uniform variables using the inverse cumulative density function assigned to each wind farm for each type of error:

$$\delta^*_{i,t,20} \equiv F_{i,20}{}^{-1}(u_{i,t,20})$$
$$\delta^*_{i,t,40} \equiv F_{i,40}{}^{-1}(u_{i,t,40})$$

The simulated errors at each virtual wind farm have the same distribution as the corresponding real wind farm. Each pair of virtual wind farms also has the rank correlation that would be expected based on their distance apart. This correlation applies when comparing the δ_{40} errors at different sites, the δ_{20} errors at different sites, or the δ_{40} and δ_{20} errors at the same or different sites.

(11) The simulated errors at all wind farms are then summed to simulate the total error at all wind farms:

$$\Delta^*_{t,40} = \sum_i \delta^*_{i,t,40}\, z_i / \sum_i z_i$$
$$\Delta^*_{t,20} = \sum_i \delta^*_{i,t,20}\, z_i / \sum_i z_i$$

The simulated variables $\Delta^*_{t,40}$ and $\Delta^*_{t,20}$ have the joint distribution that would be expected for $\Delta_{t,40}$ and $\Delta_{t,20}$ for the full set of virtual wind farms, based on their relative locations and the expected correlation between the 40-min and 20-min error statistics at each wind farm (as derived from the 10 real wind farms). (It should be noted that the simulated variables for different time steps t do not represent a chronological sequence; they simply show forecast errors that could occur during the hour before any randomly chosen minute.)

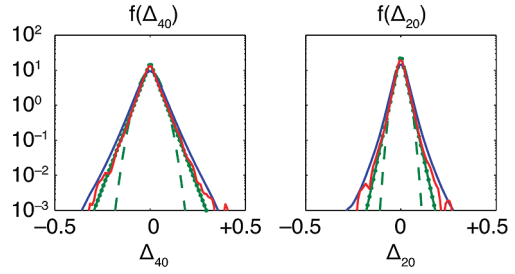

Figure 1. Simulated and observed probability densities of 40-min (Δ_{40}) and 20-min (Δ_{20}) changes in wind power production in Texas, 2006−2008. Red traces show observed values and blue traces show the simulated distribution. Green traces show Laplacian (dotted) and Gaussian (dashed) distributions with the same mean and standard deviation as the observations.

2.3. Wind Model Validation. To validate the wind variability model, I simulated $\Delta_{t,40}$ and $\Delta_{t,20}$ for all wind farms in Texas in 2006−2009, and compared the result to the actual in aggregate power output during this period.[13] This simulation used virtual wind farms identical in size and location to the actual Texas wind farms, and the virtual wind portfolio was updated as the real wind portfolio expanded from 1840 MW to 7892 MW during the 3-year period. For this simulation, only data from the six NextEra wind farms outside of Texas were used to initialize the simulation model.

Figure 1 compares kernel probability densities for the simulated and observed values of $\Delta_{t,40}$ and $\Delta_{t,20}$ during this period. The simulated values are close to the observed values, but slightly overestimate the likelihood of rare, extreme changes in wind power (the outer edges of the distribution). The green traces show the closest match that could be achieved using Gaussian or Laplacian distributions. Both of these distributions underestimate the likelihood of extreme events.

As discussed in the Supporting Information, the model tends to overestimate the likelihood of extreme events in the following 20 min when $\Delta_{t,40}$ is near zero, or when $\Delta_{t,40}$ is strongly positive or negative.

Two traits make this model a good choice for studying power system reserve requirements. (1) It tends to predict extreme events as often or more often than they actually occur, while generic models (e.g., Gaussian or Laplacian distributions) tend to underestimate the likelihood of extreme events. (2) This model works with no advance knowledge of the Texas wind farms other than their location and size. Gaussian or Laplacian models must be parametrized using the standard distribution and correlation of $\Delta_{t,40}$ and $\Delta_{t,20}$, which are generally not known in advance.

It is also unclear in advance whether the distribution of errors in a given region will be more nearly Gaussian or Laplacian. Gaussian models are valid if a power system faces independent errors from many different wind farms; however, they tend to underestimate the risk in real power systems, where forecast errors from different wind farms may be strongly correlated. In the simulation described in Section 4, small regions were found to have nearly Laplacian distributions, while larger regions had more Gaussian distributions.

3. POWER SYSTEM OPERATION

3.1. Commitment and Dispatch of Operating Reserves. Section 2 presented a statistical model of the error in forecasting wind power in a large power system. In order to assess the effect of these errors on operation of the power system, we must identify how these forecasts could be used to decide which other (conventional) power plants to use and when.

Table 1. Operating Parameters and Variable Names for Natural Gas Power Plants

	combined cycle (CC)	simple cycle (CT)
committed capacity	c_{CC}	c_{CT}
idle capacity	r_{CC}	r_{CT}
generating capacity	g_{CC}	g_{CT}
startup time (minutes)	60	20
minimum generation (% of committed capacity)	m_{CC} = 35%	m_{CC} = 35%
idle-mode emission rate (kg CO_2 per MWh)	$v_{r,CC}$ = 57	$v_{r,CT}$ = 109
generation-mode emission rate (kg CO_2 per MWh)	$v_{g,CC}$ = 382	$v_{g,CT}$ = 573

Fossil power plants need time to start up. Consequently, decisions about which plants will be used to serve loads at time t must be made before the wind power output for time t is known accurately. For this work, I identify two generic types of fossil power plant: combined cycle natural gas turbines (CC) and simple cycle natural gas combustion turbines (CT). I treat each of these resources as a homogeneous block of "capacity." At any given time, parts of the CC and CT capacity can be in either a "committed" (turned on and running) or "off" mode. The committed power plants can be in two submodes: either idle (acting as spinning reserves) or generating power. The variables used to indicate the amount of capacity in each online mode are listed in the first three rows of Table 1.

Power plants require advance notice to switch from uncommitted to committed mode. Once capacity has been committed, it can be switched between idle and generating mode very quickly. However, due to engineering and environmental restrictions, a minimum percentage of the committed capacity must always be kept in generating mode. All committed capacity generates some greenhouse gas emissions, and these are higher if the capacity is actively generating electricity.

The last four rows of Table 1 show the startup time, minimum generation level, idle-mode emissions and generating-mode emissions assumed for this study, as well as the names of variables used to refer to these factors. Startup times are conservative estimates for CC plants after an 8-h shutdown,[15] or for typical CT plants.[16] Emissions for CC and CT capacity in generation mode come from the profiles used in the U.S. National Energy Modeling System.[17] Idle-mode emissions are assumed to be 15% of the generating-mode emissions for CC plants and 19% for CT plants, in keeping with the part-load efficiency curves shown in Kim [18] for state-of-the-art plants with inlet guide vane control. A key trade-off comes from the fact that CC capacity generates lower emissions when online, but requires longer startup times than CT capacity.

This work does not consider ramp rate limitations of fossil power plants, other than the time required to startup. Katzenstein and Apt [14] show ramp rates around 40%/min for CT and 2.5%/min for CC (relative to nameplate capacity). These are much higher than the largest changes in wind power for any but the smallest regions studied in section 4 (e.g., spinning reserve requirements of 10% of wind capacity to cover 20-min forecast errors).

In this work, I estimate the emissions that could be generated if CC and CT capacity are used in concert with wind power to reliably meet a time-varying electricity load L_t.

In order to estimate the emissions due to firming up wind power separately from load and other power system contingencies, I assume that the load L_t is known in advance, and that natural gas power plants are perfectly reliable. In reality, a common pool of reserves would be used to manage all of these risks, reducing the amount needed for each one (since the three sources of uncertainty often offset each other). In power systems where the uncertainty of wind power is small compared to the uncertainty in loads or the largest possible conventional plant outage, much less reserves will need to be added to manage the uncertainty in wind power. However, in systems with very large amounts of wind power, wind output could become the dominant risk factor, and the wind-specific reserve requirements would asymptotically approach the values reported here, although they may always remain well below. Consequently, the assumptions used in this work are highly conservative for power systems with small amounts of wind power, but remain safe for power systems with any amount of wind power.

I assume a simple algorithm is used for commitment and dispatch of the fossil capacity, based on a rolling assessment of available resources and risk. At time $t-60$ min, system operators commit enough CC capacity to meet the expected load at time t ($L_t - F_{t,60}$), plus an extra spinning reserve margin s_{60}, which does not change over time. That is,

$$c_{CC,t} = (L_t - F_{t,60}) + s_{60} \quad (5)$$

where $c_{CC,t}$ is the amount of CC capacity committed at time $t-60$ to come online at time t, and s_{60} is the hour-ahead spinning reserve margin.

Equations 1, 2, and 5 can be combined to express $c_{CC,t}$ in terms of the random variables L_t, W_t, $\Delta_{t,40}$ and $\Delta_{t,20}$, and the operating parameter s_{60}:

$$c_{CC,t} = L_t - W_t + \Delta_{t,40} + \Delta_{t,20} + s_{60} \quad (6)$$

At time $t-60$, operators also ensure that they have an additional nonspinning reserve margin n_{60}, consisting of power plants that are not turned on yet but could be committed at time $t-20$ if needed to serve loads at time t. For this work, these are assumed to be existing CT plants that are available for commitment but not yet turned on. The sum of the parameters s_{60} and n_{60} must be high enough to compensate for extreme drops in wind power over the following 60 min; their values are discussed further below.

Then, at time $t-20$, system operators check the latest wind power forecast and, if needed, commit CT capacity ($c_{CT,t}$) to cover the electricity load (L_t), net of the new wind power forecast ($F_{t,20}$), plus a constant 20-min spinning reserve margin s_{20}, set high enough to compensate for the largest foreseeable drop in wind power over the next 20 min.

The amount of CT committed at time $t-20$ must meet two constraints: it cannot be more than the nonspinning reserves contracted at time $t-60$ ($c_{CT,t} \le n_{60}$), and it cannot be less than zero ($c_{CT,t} \ge 0$).

Consequently, the amount of CT capacity committed at time $t-20$ to be online by time t is as follows:

$$c_{CT,t} = \min\left\{ \begin{array}{l} \max\left\{ \begin{array}{l} L_t - F_{t,20} - c_{CC,t} + s_{20} \\ 0 \end{array} \right. \\ n_{60} \end{array} \right.$$

$$= \min\left\{ \begin{array}{l} \max\left\{ \begin{array}{l} -\Delta_{40} + s_{20} - s_{60} \\ 0 \end{array} \right. \\ n_{60} \end{array} \right. \quad (7)$$

The second line uses eqs 2 and 6 to express $c_{CT,t}$ in terms of the operating parameters s_{20} and s_{60}, and the random variable Δ_{40}.

Equation 7 indicates that generally at time $t-20$, system operators will commit enough CT generators to compensate for any change in the wind forecast since the CC generators were committed (Δ_{40}), as well as a reserve margin to cover a possible drop in wind power between time $t-20$ and t (s_{20}), less the spinning reserves already committed at time $t-60$ (s_{40}).

This strategy reduces emissions by taking a "wait and see" approach to generator commitment, making final decisions about spinning reserves at the latest possible forecast horizon (20 min in this example), when the uncertainty is relatively low compared to earlier forecast horizons. However, when the final commitment decision is made, the system always commits enough generators to compensate for the worst-case error that could occur by the time power is needed. (This model could be generalized to cover multiple forecast horizons and power technologies such as coal, hydro or load-response; however, for simplicity I only investigate a two-technology scenario in this paper.)

3.2. Risk of Power Shortfall. It is now possible to estimate the probability of running short of wind power during any randomly selected minute due to errors in the wind forecasts made 20 and 60 min before. The power system will run short of power during minute t if and only if the load minus wind power production is greater than the amount of CC and CT generation committed at $t-60$ and $t-20$, respectively. So the average risk of power shortfall, as a function of the operating parameters s_{60}, s_{20}, and n_{60} is as follows:

$$R(s_{60}, s_{20}, n_{60}) = \frac{\sum_t \left\{ \begin{array}{ll} 1 & \text{if} L_t - W_t > c_{CC,t} + c_{CT,t} \\ 0 & \text{otherwise} \end{array} \right.}{\sum_t 1} = \frac{\sum_t \left\{ \begin{array}{ll} 1 & \text{if} s_{60} + \Delta_{40} + \Delta_{20} + \min\left\{ \begin{array}{l} \max\left\{ \begin{array}{l} -\Delta_{40} + s_{20} - s_{60}, \\ 0 \end{array} \right\}, \\ n_{60} \end{array} \right\} < 0 \\ 0 & \text{otherwise} \end{array} \right.}{\sum_t 1} \quad (8)$$

Note that this does not consider the possibility of running short of power because too little generation capacity has been built or because of unexpected outages at nonwind power plants. It focuses only on operational decisions in a system with sufficient resources available.

3.3. Emissions Impacts of Forecast Errors. In order to estimate the emissions that come from using fossil plants to compensate for wind forecast errors, we must know how often gas capacity will be used to generate electricity and how often it will be committed but idling. For this work, I assume that dispatch follows a simple set of rules, in order: (1) all CT capacity committed for time t must generate at least its minimum required level of power (column 5 of Table 1) (For simplicity I

assume that loads are always high enough to keep CC production above its minimum level. This assumption does not affect reliability, since wind can be curtailed in order to maintain CC generation above its minimum level. However, it does omit the emissions that occur during occasional periods when gas power is kept on by the minimum-generation constraint.); (2) committed CC capacity will be dispatched (switched from idle to generation mode) to satisfy the remaining load, until all committed CC capacity is exhausted; (3) CT capacity will be dispatched to satisfy any remaining load, up to the total amount of committed CT capacity. This gives the following equations for power generation by CC and CT plants at time t.

$$g_{CC,t} = \min\begin{cases} L_t - W_t - g_{CT,t} \\ c_{CC,t} \end{cases} = \min\begin{cases} L_t - W_t - g_{CT,t} \\ L_t - W_t + s_{60} + \Delta_{40,t} + \Delta_{20,t} \end{cases} \quad (9)$$

$$g_{CT,t} = \max\begin{cases} \min\begin{cases} L_t - W_t - c_{CC,t} \\ c_{CT,t} \end{cases} \\ m_{CT} c_{CT,t} \end{cases} = \max\begin{cases} \min\begin{cases} -\Delta_{40,t} - \Delta_{20,t} - s_{60} \\ c_{CT,t} \end{cases} \\ m_{CT} c_{CT,t} \end{cases} \quad (10)$$

The second version of each equation is found using eq 6.

We can also estimate the amount of generation capacity that is online but idle (not actively generating power) at each time t:

$$r_{CC,t} = c_{CC,t} - g_{CC,t} \quad (11)$$

$$r_{CT,t} = c_{CT,t} - g_{CT,t} \quad (12)$$

It is now possible to estimate the emissions associated with firming up wind power for use in the electricity system. These "excess emissions" can be defined as the difference between the emissions when running a combination of wind, CC and CT plants using the rules above, and those expected when running a CC plant alone to meet the loads. If wind power directly displaced CC operation, then the emission savings would be equal to the wind power output, multiplied by the generation emission rate of CC plants. However, in reality some of these emission savings are reversed when the system commits additional CC or CT capacity to compensate for the risk of falling wind power, or dispatches inefficient CT capacity because insufficient CC capacity was committed in advance.

Excess emissions, as a fraction of the expected emission savings due to wind power are calculated as follows:

$$E = \frac{\sum_t \nu_{g,CC} g_{CC,t} + \nu_{g,CT} g_{CT,t} + \nu_{r,CC} r_{CC,t} + \nu_{r,CT} r_{CT,t} - (L_t - W_t)\nu_{g,CC}}{\nu_{g,CC} \sum_t W_t}$$
$$\approx \frac{\sum_t (\nu_{g,CT} - \nu_{g,CC}) g_{CT,t} + \nu_{r,CC} \max(g_{CT,t} + \Delta_{40,t} + \Delta_{20,t} + s_{60}, 0) + \nu_{r,CT}(c_{CT,t} - g_{CT,t})}{\nu_{g,CC} \sum_t W_t} \quad (13)$$

The second version of this equation is obtained via eqs 6, 9, 11 and 12, but with a simplification that ignores the emissions "savings" that could occur when the system fails to commit enough CC and CT capacity to satisfy the load unmet by wind. The full derivation of the second equation is shown in the Supporting Information.

Noting the definitions of $c_{CT,t}$ and $g_{CT,t}$ in eqs 7 and 10, it is clear that in this formulation the excess emissions, E, depend only on the emission coefficients for each power plant in each mode ($\nu_{g/r,CC/CT}$ from Table 1), the operating reserve targets (s_{60}, s_{20}, and n_{60}), the random forecast errors ($\Delta_{t,40}$ and $\Delta_{t,20}$), and the average power production from the wind farms in the region ($\Sigma_t W_t / \Sigma_t 1$). In particular, this model does not depend on the specific level of load or wind at any time, because reserve targets are assumed to be constant at all times and the model ignores the emission consequences of (rarely) shedding load due to under-commitment of CC and CT or curtailing wind due to over-commitment of CC.

Before proceeding, it should be noted that this model focuses on the reduction of emissions from the ongoing operation of power plants. It does not address the effect of wind power on the frequency of starts and stops for natural gas power plants. Although this model makes commit/decommit decisions for CC and CT capacity every minute, the actual operation of these plants does not vary sharply up and down. Generally, CC plants are scheduled to follow the hour-to-hour changes in wind, and CT plants are only committed when there are unusually large declines in wind power output.

This model also does not address the fact that power plants must be committed in discrete quantities—if the system needs an additional 50 MW committed at any point, then it must commit a full generator unit, which may be on the order of 200−400 MW. On average, an extra half of a generator would be expected to be committed at any time. However, this overcommitment should be the same whether or not wind power is included in the system.

4. RESULTS

I used the model described above to estimate the emissions from wind farms dispersed across regions of various sizes. This analysis proceeded as follows:

(1) Define several sets of virtual wind farms whose forecast errors will be simulated. For this work, I use the locations and sizes of potential eastern-U.S. wind farms modeled in the Eastern Wind Integration and Transmission study.[5] I perform the analysis nine times, using increasingly large subregions, as shown by the black rings in Figure 2.

(2) Use the statistical model to simulate 10^7 instances of $\Delta_{t,40}$ and $\Delta_{t,20}$ for each of the modeled regions (equivalent to 19 years of wind errors, reported every minute).

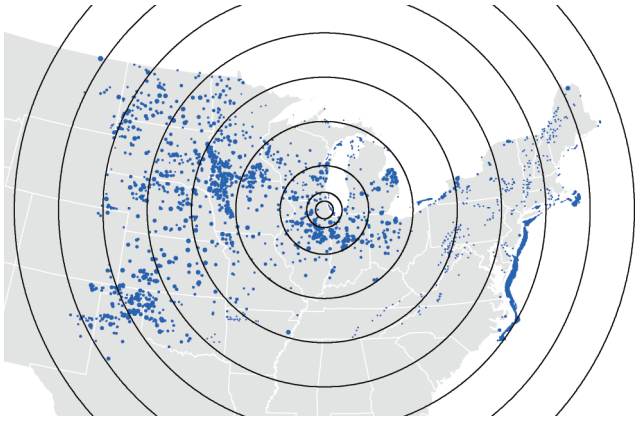

Figure 2. Location of virtual wind farms used for this study. Blue dots indicate wind farm locations (gradated by size), and black rings show the subsets simulated for this study (regions with diameters of 100, 200, 500, 1000, ..., 3500 km).

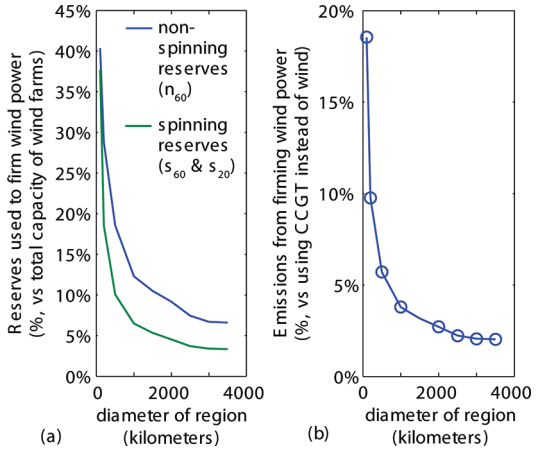

Figure 3. (a) Reserves used to firm wind power and (b) and emissions due to these reserves, relative to direct emission savings of wind power (both for regions 100−3500 km across).

(3) Set the nonspinning reserve margin n_{60} equal to 100% of wind capacity in the region; set the spinning reserve margins s_{60} and s_{20} equal to each other, and adjust them until the risk R for the region (eq 8) is 0.000009 (just below 0.00001). Setting s_{60} and s_{20} equal to each other generally achieves the lowest possible emissions for any level of risk, ensuring that enough CC generators are turned on 60 min ahead to meet the final 20-min spinning reserve margin (setting s_{60} higher than s_{20} tends to result in commitment of unneeded CC capacity, and setting it lower leads to commitment of less-efficient CT instead of CC).

(4) Freeze s_{60} and s_{20} and adjust n_{60} down until the risk level R is 0.00001. This corresponds to about 50 min of generation shortfall every 10 years, which is similar to the reliability goals of existing power systems. This provides a full set of reserve targets, which can be used to assess the emissions that may occur as a result of dynamically firming up wind power with natural gas plants while maintaining a satisfactory risk level.

(5) Estimate the excess emission rate E for each subregion using eq 13 with the simulated values from step 2 and the operating parameters from step 4.

Figure 3(a) shows the nonspinning and spinning reserves allocated for each subregion. For power systems with wind farms dispersed across a 500 km or larger area, it should be possible to firm up wind with 10% or less spinning reserves and 20% or less nonspinning reserves (both relative to the total rated capacity of the wind farms). (These are both upper limits, based on the conservative assumptions described above). It is also possible to integrate wind using less nonspinning CT capacity if the 60-min spinning reserves target is raised, but this strategy will increase emissions somewhat. The optimal balance between spinning and nonspinning reserves depends on the amount of CT capacity already available and the relative cost of fuel and emissions vs CT capacity.

It should also be noted that wind power is generally added to systems that already have enough conventional plants to meet their peak electricity loads, so there is no need to build additional reserves specifically to complement wind. However, wind development may be constrained in systems that have limited flexible generation resources (e.g., heavy dependence on coal or nuclear power).

Figure 3(b) shows the emissions from the operation of reserve plants to compensate for the uncertainty of wind power forecasts. These are shown as a fraction relative to the emission savings that would occur if wind power directly displaced CC generation with no need for operating reserves. Alternatively, the plot can be interpreted as the net emission rate of firmed-up wind power when compared to a CC plant.

When wind power is dispersed across regions larger than about 500 km across, 6% or less of their emission savings are reversed by the reserve power operations. This is much less than the 20% reported by Katzenstein and Apt [9] for full-time, 100% backup of individual wind farms.

It should also be noted that this is an *upper* limit on the expected emissions; emissions will be lower if the uncertainty of wind forecasts is small compared to other uncertainties in the system, or if better wind forecasts are used, or if operating reserves are provided by lower-emission or faster-starting resources (e.g., hydropower or load response, which create no direct emissions).

5. DISCUSSION

This work introduces a new model to estimate the range of possible errors in forecasts of wind power production in regions of various sizes. An example is also given of using this model with a simplified power system model to estimate the amount of greenhouse gas emissions that could be released when natural gas power plants are assigned to compensate for 99.999% of wind forecast errors. This power system model uses "worst-case" assumptions—that dedicated reserves are used for wind power separately from other sources of uncertainty in the system—and so it estimates an *upper limit* on the emissions that could occur. Emissions are likely to be significantly lower in power systems where wind is not the dominant source of uncertainty.

Two key conclusions emerge from this work:

(1) The larger the area over which wind farms are dispersed, the lower the burden is likely to be for firming the supply of wind power; and

(2) For large regions (500 km or more across), the emissions due to firming of wind power are likely to be low, less than 6% of the emissions that would have been generated if CC

plants had provided the power instead of wind farms. These emissions are due primarily to running excess CC plants (expending energy to keep idle capacity online), and to a much smaller degree to running excess CT plants or generating power from inefficient (but fast-starting) CT plants instead of more efficient CCGT plants.

These conclusions imply that in large power systems, producing power in wind farms will cause at least 94% less CO_2 emissions than producing the same amount of power with natural gas. However, to make best use of wind power, more flexible market rules may be needed to take advantage of the fastest-start capabilities of reserve power plants, e.g., rolling 5-min markets for reserves instead of hour-ahead or day-ahead. The later decisions can be delayed about committing spinning reserves, the fewer will need to be committed, and the lower costs and emissions will be.

This work has not addressed several other options for providing operating reserves with potentially lower emissions than the approach studied here. Other possibilities may become more attractive as wind makes up a larger share of the power system: addition of superpeaking capability to CC or CT plants, so they can quickly provide more power without waiting for another plant to start up; taking advantage of the fact that CC and CT plants *begin* to supply power within a few minutes of startup instructions, well before they reach full power; short-term demand-response (e.g., cycling air conditioners or refrigerators off for a few minutes at a time),[19] and zero-emission reserve sources such as hydro power, flywheels, or ultracapacitors. The unit commitment method presented in this work is mostly constrained by the start time of the *fastest* units in the system, so the addition of even small amounts of fast-start capacity could make a large difference.

Finally, it should be noted that this model represented a simplified power system with natural gas capacity at least equal to the wind capacity. Different results are likely to be found in systems with different resource mixes: coal plants have higher emissions than gas but longer unit commitment delays; hydro-based systems can integrate wind more easily, but may have fewer emissions to avoid. This work has also assumed that ample transmission capacity is available to move reserves throughout the region; in reality there may be trade-offs between the cost of transmission upgrades, vs losses on long-distance lines, vs reductions in reserve requirements.

■ ASSOCIATED CONTENT

Ⓢ Supporting Information. Details on the existing wind farms used to parametrize this model; a figure showing the rank correlation between wind farm forecast errors as a function of distance; additional validation figures and data for the wind forecast error model; a discussion of the idle- and generation-mode emission coefficients; a derivation of the excess emissions equation; and the Matlab code for the models. This material is available free of charge via the Internet at http://pubs.acs.org.

■ AUTHOR INFORMATION

Corresponding Author
*E-mail: matthias.fripp@eci.ox.ac.uk.

■ ACKNOWLEDGMENT

Thanks to Mike Slattery, Nick Eyre, and three anonymous reviewers for insightful questions and advice. Thanks to several NextEra Energy Resources staff for wind farm data and industry insight, especially Skelly Holmbeck, Mark Mango, Mark Ahlstrom, Peter Wybierala, and Matt Schafer. NextEra Energy Resources funded this research, but the findings were not subject to review or approval by the company.

■ REFERENCES

(1) CRA *SPP WITF Wind Integration Study*; Charles River Associates for Southwest Power Pool: Boston, MA, January 4, 2010.

(2) NYISO *Growing Wind: Final Report of the NYISO 2010 Wind Generation Study*; New York Independent System Operator: Rensselaer, NY, September, 2010.

(3) GE Energy *Western Wind and Solar Integration Study*; National Renewable Energy Laboratory: Golden, CO, May, 2010; p 535.

(4) EWIS *European Wind Integration Study*; European Wind Integration Study: Brussels, March 31, 2010.

(5) EnerNex Corporation *Eastern Wind Integration and Transmission Study*; National Renewable Energy Laboratory: Golden, CO, January, 2010; p 241.

(6) Porter, K.; IAP Team *Intermittency Analysis Project: Final report*; CEC-500−2007−081; California Energy Commission: Sacramento, CA, July, 2007; p 71.

(7) Holttinen, H.; Meibom, P.; Orths, A.; Hulle, F. v.; Lange, B.; O'Malley, M.; Pierik, J.; Ummels, B.; Tande, J. O.; Estanqueiro, A.; Matos, M.; Ricardo, J.; Gomez, E.; Söder, L.; Strbac, G.; Shakoor, A.; Smith, J. C.; Milligan, M.; Ela, E. *Design and operation of power systems with large amounts of wind power; Final report, IEA WIND Task 25, Phase one 2006−2008*; VTT Tiedotteita − Research Notes 2493; VTT Technical Research Centre of Finland: 2008.

(8) Weber, C. Adequate intraday market design to enable the integration of wind energy into the European power systems. *Energy Policy* **2010**, *38* (7), 3155–3163.

(9) Katzenstein, W.; Apt, J. Air emissions due to wind and solar power. *Environ. Sci. Technol.* **2008**, *43* (2), 253–258.

(10) Mills, A.; Wiser, R.; Milligan, M.; O'Malley, M. Comment on "Air emissions due to wind and solar power." *Environ. Sci. Technol.* **2009**, *43* (15), 6106–6107.

(11) Higham, N. J. Computing the nearest correlation matrix--a problem from finance. *IMA J. Numer. Anal.* **2002**, *22* (3), 329–343.

(12) Li, S. T.; Hammond, J. L. Generation of pseudorandom numbers with specified univariate distributions and correlation coefficients. *IEEE Trans. Syst. Man Cybernet.* **1975**, *SMC-5* (5), 557–561.

(13) Wan, Y.-h. *Summary Report of Wind Farm Data: September 2008*; National Renewable Energy Laboratory: Golden, CO, May, 2009.

(14) Katzenstein, W.; Apt, J. Air emissions due to wind and solar power: Supporting information. *Environ. Sci. Technol.* **2008**, *43* (2), 253–258.

(15) Kehlhofer, R.; Rukes, B.; Hannemann, F.; Stirnimann, F., *Combined-Cycle Gas and Steam Turbine Power Plants*. 3rd ed. ed.; PennWell Books: Tulsa, OK, 2009.

(16) Angello, L. *Advanced Monitoring to Improve Combustion Turbine/Combined Cycle CT/(CC) Reliability, Availability and Maintainability (RAM); Semi-Annual Report* Agreement Number DE-FC26−01NT41233; Electric Power Research Institute: Palo Alto, CA, April 1−September 30, 2004.

(17) EIA *Assumptions to the Annual Energy Outlook 2010*; DOE/EIA-0554(2010); Energy Information Administration, U.S. Department of Energy: Washington, DC, April 9, 2010.

(18) Kim, T. S. Comparative analysis on the part load performance of combined cycle plants considering design performance and power control strategy. *Energy* **2004**, *29* (1), 71–85.

(19) Kirby, B. J. *Spinning Reserve from Responsive Loads*; ORNL/TM-2003/19; Oak Ridge National Laboratory: Oak Ridge, TN, March, 2003.